Onset of Scattering Induced Miniband Transport

C. Rauch, G. Strasser, and E. Gornik
Institut für Festkörperelektronik und Mikrostrukturzentrum der TU Wien, Technische Universität Wien, Floragasse 7, A-1040 Wien, Austria

A systematic study of electron transport in undoped GaAs/GaAlAs superlattices is presented. Hot electron spectroscopy is used to measure the superlattice transmittance at different bias conditions. The transmittance of a five period superlattice is found to be independent of the direction of the electric field, while for a superlattice larger than ten periods, a dependence of the transmission on the electric field direction is observed. The onset of scattering induced miniband transport is clearly evident. From the experimental data a coherence length of 150 nm is derived. The limiting mechanism is found to be interface roughness scattering.

1. Introduction

Decreasing the barrier thickness of multiple quantum well structures leads to a stronger coupling between the degenerate eigenstates in the wells and thus to the formation of superlattice minibands. The application of an external electric field parallel to the growth axis quantizes the energy continuum associated with the miniband dispersion into a Stark ladder of discrete energy levels, and transforms the extended Bloch waves into strongly localized wave functions. Under strong localization coherence will be reduced to a few periods and in the limit, to a single quantum well.

Numerous studies of the formation of superlattice minibands have been reported including transport measurements of biased n-i-n superlattice structures. However, it turns out that the experimental study of electronic properties of a biased superlattice is hindered by the interdependence of the intensity of the current injected and the field present in the superlattice [1]. At high electric fields the large current densities make the field in the superlattice non-uniform and causes the formation of high field domains and leads to thermal saturation of miniband transport [2].

In this work we present a study of ballistic transport in nominally undoped GaAs/ $Ga_{0.7}Al_{0.3}As$ superlattices, where the influence of electron-electron and electron-impurity scattering can be neglected. Under flat band conditions the eigenstates of the periodic structure are expected to be extended over the entire length of the superlattice. We apply the technique of hot electron spectroscopy to measure the positions of the minibands and to investigate the transmission of hot electrons in biased superlattices.

2. Experiment

A three terminal device is used to probe the transmittance of undoped GaAs/GaAlAs superlattices. An energy tunable electron beam is generated by a tunneling barrier and passes the superlattice after traversing a thin highly doped n-GaAs base layer and an undoped drift region. The measured collector current reflects the probability of an injected electron to be transmitted through the superlattice. The transmittance of the superlattice can be measured directly at given superlattice bias conditions by varying the energy of the injected hot electrons independent from the superlattice bias.

Our samples, grown by molecular beam epitaxy, have the following common features: A highly doped n^+-GaAs collector contact layer ($n = 1x10^{18}$ cm^{-3}) is followed by a superlattice and the drift regions which are slightly n-doped ($5x10^{14}$ cm^{-3}). This is followed by a highly doped ($2x10^{18}$ cm^{-3}) n^+-GaAs layer (base) of 13 nm width. On top of the base layer a 13 nm undoped $Ga_{0.7}Al_{0.3}As$ barrier is grown followed by a spacer and a n^+-GaAs layer, nominally doped to $n = 3x10^{17}$ cm^{-3}, in order to achieve an estimated normal energy distribution of injected electrons of about 20 meV. Finally, a n^+-GaAs contact layer ($n = 1x10^{18}$ cm^{-3}) is grown on top of the heterostructure to form the emitter.

In Fig. 1 the calculated conduction band diagram is shown for typical bias conditions. The miniband positions (indicated by shaded areas) are calculated using a self consistent Schrödinger calculation. The static transfer ratio $\alpha = I_C/I_E$ of a five period superlattice with 2.5 nm AlGaAs barriers and 8.5 nm GaAs wells is plotted as a function of the injection energy. The position of the first peak coincides very well with the calculated position of the first miniband. The second observed peak is shifted 36 meV to higher injection energies and is ascribed to the first LO-phonon emission replica ($\hbar\omega_{LO}$ = 36 meV) of the injected electron distribution. The peak at 150 meV represents transport through the second superlattice miniband, and the sharp rise of the transfer ratio at 280 meV is due to the transition to continuum.

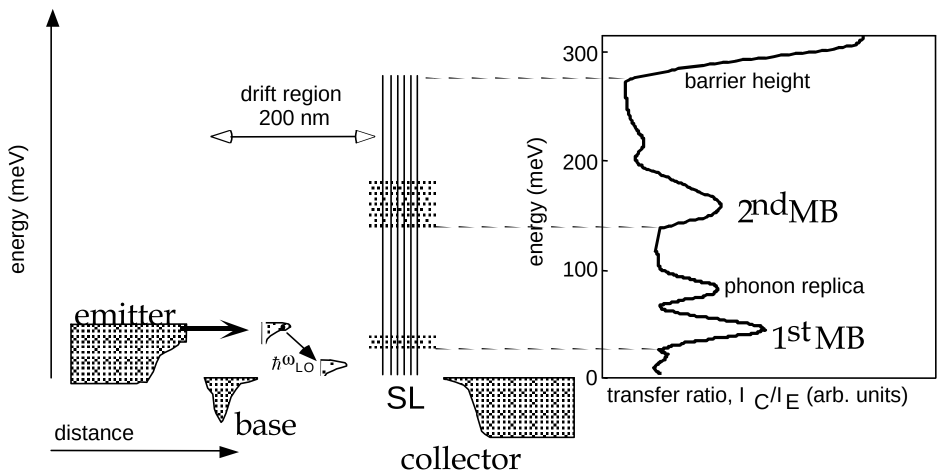

Fig. 1: Calculated conduction band diagram along the growth direction. The transfer ratio of a 5 period superlattice with 2.5 nm barriers and 8.5 nm wells is plotted vs. injection energy.

The measured static transfer ratio of a 5 period superlattice with 2.5 nm AlGaAs barriers and 6.5 nm GaAs wells versus injection energy is shown in Fig. 2 for different collector biases. The black solid line represents the transfer ratio at flat band condition (U_{BC} = 0). The sharp increase of the transfer ratio at about 45 meV coincides very well with the lower edge of the first miniband which is calculated to be 46 meV. A clear shift of the maximum (due to the voltage drop in the drift region) and a reduction of the amplitude of the transfer ratio is observed for increasing collector voltages.

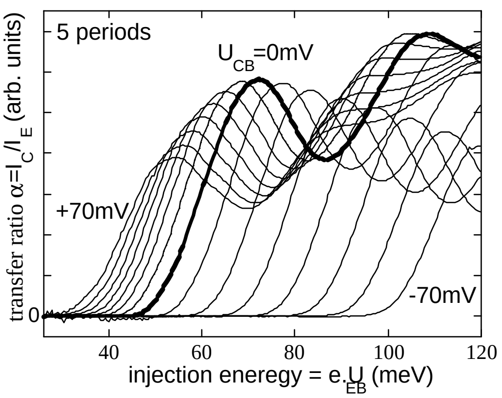

Fig. 2: Transfer ratio versus injection energy at different collector base voltages of a 5 period superlattice with 6.5 nm GaAs well and 2.5 nm AlGaAs barriers. The solid black line represents the transfer ratio under flat band condition (U_{BC} = 0).

In order to investigate the transmission of biased superlattices we have taken the total miniband transmission (T_α) which is defined as twice the area of the lower energy side of the first transfer ratio peak as a measure for the average current through the first miniband at given bias conditions. The analysis of T_α versus applied electric field for the five and 20 period superlattices is shown in Fig. 3. The total miniband transmission T_α (dots) of the 5 period sample is symmetric for both bias directions, while clear asymmetric behavior is observed for the 20 period sample (diamonds).

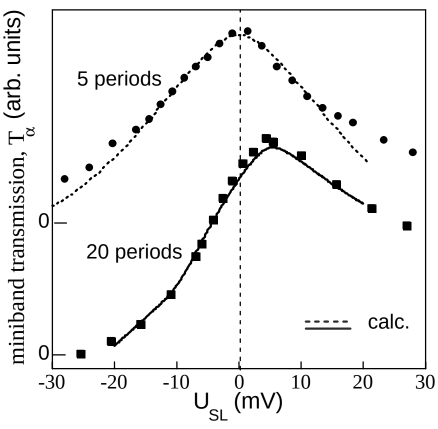

Fig. 3: Miniband transmission versus electric field of the 5 and 20 period superlattice compared to a one- and three-dimensional calculation respectively.

To understand our findings we have performed two different kinds of calculations for the transmission through the superlattice. In a first calculation, based on a transfer matrix method, we consider a 1-dimensional ideal structure with nominal sample parameters. The calculated coherent transmission T_α (dashed line) is in good agreement with the experiment for the 5 period sample as shown in Fig. 3, demonstrating that the transport is dominated by coherent transmission in this case.

However, the picture changes dramatically for the 20 period structure: For negative bias (decelerating field) the measured current decays much faster with field than the one predicted by the 1-dimensional calculation. For positive bias the current first increases slightly until it decays rapidly but always stays higher than the calculated coherent model.

We assign the observed difference between the 20 and 5 period superlattice to the onset of diffusive transport. For a longer superlattice only a small fraction of the carriers can traverse the structure without scattering. Typically, the scattering process decreases the kinetic electron energy in the transport direction, either by transferring the energy difference to a motion perpendicular to the superlattice-direction (elastic scattering), or by exciting a phonon (inelastic). If a positive bias is applied to the collector, we observe an increase of the transfer ratio since the scattered electrons contribute additionally with the coherent electrons to the collector current. For the negative bias only coherent electrons traverse the superlattice, scattered electrons are flowing back to the base according to the applied electric field. Therefore the presence of scattering destroys the symmetry of the transmission with respect to the field direction. The transition from coherent to diffusive transport is clearly evident.

In order to check this reasoning the results were compared with a second calculation of the transmission through a full 3-dimensional structure where interface roughness is included [3]. As shown in Fig. 3, the calculated transmission (solid line) becomes asymmetric in excellent agreement with the experimental result (diamonds) indicating the limitation of the coherence length due to interface roughness scattering.

Following our reasoning given above, the transmission for negative fields is mainly due to the fraction of electrons traversing the structure without scattering. The average velocity in the miniband is of the order of $\Delta d/(2\hbar) = 1.5 \times 10^7$ cm/s where d is the superlattice period and Δ the miniband width. Using this value in a mean free path of $\ell_{coh} = v\tau_{scatt}$ =150 nm, which is one of the longest reported so far.

In summary, we have used hot electron spectroscopy to investigate the transmission of biased undoped superlattices. The onset of scattering induced miniband transport has been observed and the coherence length has been determined to be 150 nm. We have shown that the coherent transport at 4.2 K is limited by interface roughness scattering.

References

[1] F. Beltram, et al., Phys. Rev. Lett. **64**, 3167 (1990).

[2] G. Brozak, et al., Phys. Rev. Lett. **64**, 3163 (1990).

[3] C. Rauch, et al., Phys. Rev. Lett. **81**, 3495 (1998).